T.3: Study of carbon removal from synchrotron mirror like gold surfaces using different techniques

Praveen Kumar Yadav[*,1] **and Mohammed H. Modi**[1,2]
[1]*Synchrotrons Utilization Section, RRCAT, Indore*
[2]*Homi Bhabha National Institute, Mumbai*
[*]*Email: praveenyadav@rrcat.gov.in*

Abstract
Synchrotron radiation (SR) induced carbon contamination on optical elements is a serious issue in SR beamlines. Carbon contamination reduces photon flux by scattering and absorption near carbon K-edge region. The deposited carbon layer causes interference fringes in total external reflection region of gold/platinum coated reflective optics. To retain the beamline performance the carbon contaminated optics should be refurbished by a suitable technique. In literature, three suitable techniques (radio frequency (RF) plasma, ultraviolet (UV) radiation (λ=172 nm) and infra-red (IR) laser (λ=1064 nm) exposure) are reported to remove carbon contamination from optical elements. Selection of a technique for optics cleaning depends on the nature of carbon layer (graphitic, diamond like carbon, etc.). In the present study, we have applied all the three surface cleaning techniques independently for removal of carbon contamination from gold surface and detailed surface characterizations are carried out using soft x-ray reflectivity (SoXR), x-ray photoelectron spectroscopy (XPS), Raman spectroscopy (RS) and atomic force microscopy (AFM) techniques. Characterization results suggest that all the three techniques are capable of removing carbon contamination with certain limitations. Here detailed relative effects on gold surface after cleaning experiments with the three techniques are discussed.

1. Introduction

High brilliance, coherence and stability of synchrotron radiation sources make them powerful tool for research in the field of fundamental and applied science [1]. High brilliance sources have imperative requirement of high quality optics to preserve wave-front characteristics while transporting high photon flux ($10^{12\text{-}13}$ ph/s) from source point to the experimental station [2]. Due to prolonged use, optical elements such as mirrors, gratings and transmission filters are subject to buildup of carbon contamination by dissociation and subsequent cross-linking of carbon containing molecules adsorbed on the surface of optics. Dissociation of the adsorbed molecules takes place by primary SR photons [3] as well as by secondary electrons [4] generated on the mirror surface. The exact process of carbon deposition is more complex in which surface diffusion of hydrocarbon molecules towards SR illuminated area also contributes [3]. The actual form of carbon deposited on optical elements after dissociation of hydrocarbon molecules by SR beam is also not well known because the properties of the contamination layer vary with photon dose, the amount of hydrogen present and relative contribution of different hybridization states (sp^3, sp^2 and sp^1) of carbon in the layer structures. Ferrari & Robertson [5] explained different phases of carbon by the presence of sp^2, sp^3 and H contents using ternary phase diagram.

The reflectivity loss from an optical element strongly depends on nature of carbon layer deposited. Due to high density of diamond like carbon (sp^3) film the reflectivity loss is higher compared to graphitic-like carbon (sp^2). This carbon layer on mirrors reduces the photon flux near the carbon K-absorption edge (284 eV). In the case of multi-element optical systems, even a very thin layer of carbon on top of each optical element reduces the reflected photon flux significantly. Figure T.3.1 shows the measured reflectivity spectrum (50 eV to 320 eV) of carbon contaminated (40 nm) Au mirror compared with calculated Au mirror. The reflectivity spectrum of carbon contaminated mirror clearly shows strong reflectivity loss (82% to 25%) near carbon K-edge (284 eV) due to absorption of incident photons by carbon atoms whereas without carbon layer the mirror shows more than 60% reflectivity in carbon K-edge region.

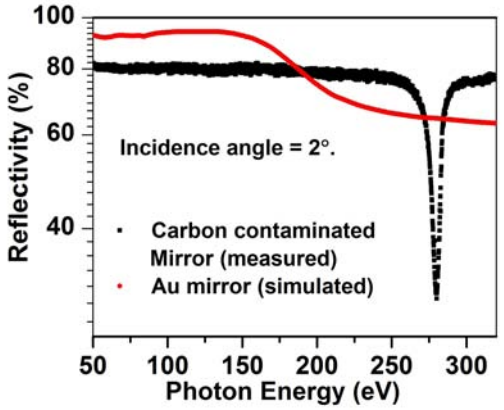

Fig. T.3.1: Comparison of soft x-ray reflectivity of carbon contaminated Au mirror with pristine Au mirror near carbon K edge region.

This additional carbon layer produces a phase difference which leads to destructive interference at certain wavelengths. The resultant reflected intensity pattern of SR beam from carbon contaminated mirror will vary as carbon layer thickness changes. Figure T.3.2 shows the effect of carbon layer thickness on reflectivity due to the interference effect in 300 eV to 2 keV energy region.

In previous studies it is observed that the deposited carbon layer has high surface roughness [6], [7]. Increase in surface roughness due to carbon deposition also exponentially decreases the reflected photon flux [$R=R_0 \exp(-q^2\sigma^2)$] where R_0 is the reflectivity of smooth surface and q and σ are the momentum transfer perpendicular to surface and rms surface roughness, respectively.

Figure T.3.3 shows the effect of surface roughness of carbon layer on reflectivity. The spectra show the simulated reflectivity of Au mirror at 2.5 degree incidence angle in 300 eV to 2 keV energy range without carbon layer and with carbon layer of different roughness. These results suggest that carbon contamination on optical elements limits beamlines performance due to increase in absorption, interference, and scattering effects.

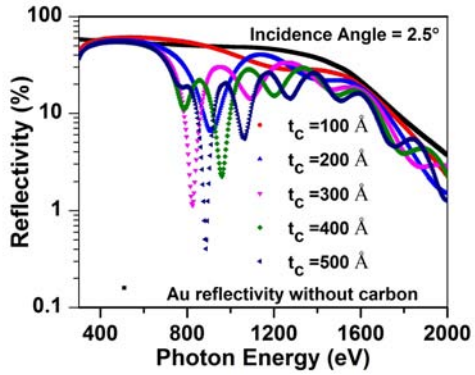

Fig. T.3.2: Effect of carbon layer thickness (t_c) on x-ray reflectivity of carbon contaminated Au mirror in 300 eV to 2 keV energy range at 2.5 degree incidence angle.

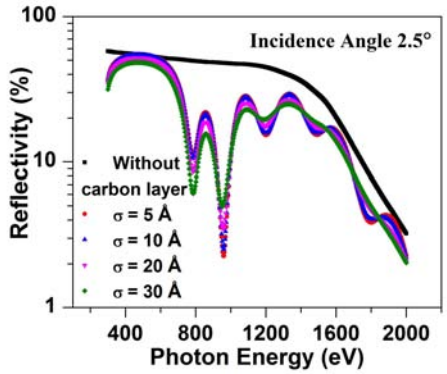

Fig. T.3.3: Effect of surface roughness (σ) on X-ray reflectivity of carbon contaminated Au mirror is shown.

The performance of beamline can be maintained by periodic refurbishment of optical elements using suitable technique. Before applying the carbon removing technique it is better to determine the phase/structure of carbon layer. The denser structure of DLC film is likely to be more difficult to remove by the UV/O_3 cleaning method because the carbon in DLC form is more tightly bound. Different online and offline techniques are investigated for cleaning contaminated optics. In this article the results of characterization of SR induced carbon layer deposited on Au coated toroidal mirror and LiF window surface are briefly discussed. Details of in-house developed refurbishment techniques viz. RF plasma, UV radiation (λ=172 nm) and IR laser techniques along with result of carbon cleaning experiments are discussed.

2. Characteristics of synchrotron radiation induced carbon

We have taken two SR induced carbon contaminated samples, the first one is Au coated toroidal pre mirror (TM1) of soft x-ray reflectivity beamline [8] of Indus-1. The beamline optical layout and position of TM1 is shown in Figure T.3.4. The beamline is in operation since the year 2001 and it is maintained in ~ 10^{-9} mbar vacuum regime. TM1 of the beamline is exposed to high photon flux of wavelengths covering from infrared to soft x-ray region. TM1 accepts SR beam 10 mrad in horizontal direction and 5.9 mrad in vertical direction.

At 450 MeV electron energy and 100 mA ring current the maximum radiated SR beam power from Indus-1 in 10 mrad acceptance of mirror is about 577 mW, to which TM1 is exposed.

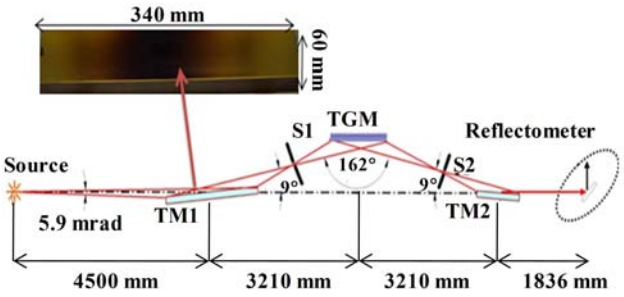

Fig. T.3.4: Optical layout of the reflectivity beamline, Indus-1 is shown alongwith carbon contaminated Au coated pre-mirror. TGM, TM1 and TM2 represent toroidal grating monochromator, pre and post focusing mirrors, respectively. S1 and S2 represent entrance and exit slits.

The second sample is carbon contaminated LiF window (shown in Figure T.3.5), which is used as low pass filter and isolates the experimental station from rest of the beamline in HRVUV beamline [9] of Indus-1 SR source.

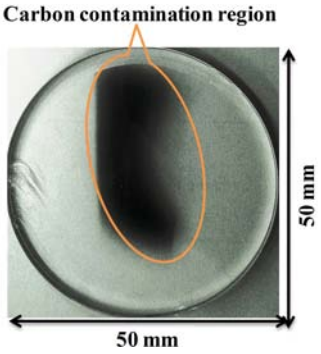

Fig. T.3.5: Carbon contaminated LiF window, marked area in photograph indicates contamination region.

In this case, the carbon contamination layer was deposited in a short time exposure of about 100 hrs with photons of 3 eV to 11.5 eV energy that are transmitted through the LiF window. Pressure in the beamline towards experimental station was ~10^{-6} mbar and towards the storage ring side it was ~10^{-9} mbar, carbon contamination layer deposited on the face of high pressure regime. Here we briefly introduce the SR induced carbon characteristics. Detailed characterization results are discussed in earlier publications [6], [10]. Carbon in the contamination layer is found in both sp^3 and sp^2 hybridized states and its properties vary with the incident photon dose. The carbon on the mirror surface is in the form of small clusters, the size of the clusters increases with photon dose. Our Raman results suggest that in high photon dose region, I(D)/I(G) ratio and D- peak width is high which indicates that the number of rings in the cluster and disordering in the cluster increases. The ratio of the slope (m) of the linear background of Raman spectrum to the intensity of the G-peak [m/I(G)] reveals that in contamination layer, the hydrogen content decreases

with photon dose. These results suggest that the SR induced carbon is hydrogenated graphitic carbon and dispersed on mirror surface in form of small clusters. From SoXR analyses it comes out that the optical density of carbon layer deposited on Au mirror surface is 75% and on LiF window surface it is 94% of graphitic carbon.

3. Carbon cleaning techniques

In the present study we have applied RF plasma, UV radiation (λ=172 nm) and IR laser (λ=1064 nm) exposures techniques independently for removal of carbon contamination from gold surface and detailed surface characterizations are carried out using SoXR, XPS, Raman spectroscopy and AFM techniques. Here detailed relative effects on gold surface after cleaning experiments with three techniques are discussed.

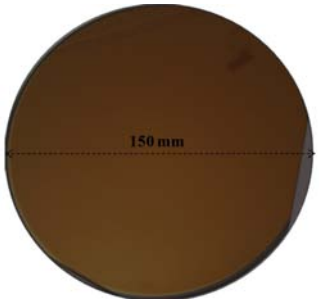

Fig. T.3.6: Graphitic carbon deposited on gold coated silicon wafer of 150 mm diameter was used as a test sample for carbon cleaning experiments.

Since the nature of SR induced carbon closely matches with the graphitic carbon [6], [7], [10] therefore a thin film of graphitic carbon was deposited on a large size gold coated silicon wafer (Φ=150 mm) using ion beam sputtering (sample is shown in Figure T.3.6) and then small size pieces of samples were cut from this big size sample and used for carbon cleaning experiments using three different techniques. For improving the adhesion between the silicon substrate and the gold layer a seeding layer of chromium was deposited. The layer structure of sample is Si-substrate/Cr-75Å/Au-730Å/C-180Å (numerical values represent thicknesses of different layers).

3.1 Description of carbon removing techniques

3.1.1 Capacitively coupled RF plasma setup

In order to remove carbon from Au surface using RF plasma exposure a ~20 mm × 40 mm sample was used (mentioned in sec. 3). For plasma exposure an in-house developed system is used [11]. The RF plasma system is capacitively coupled and equipped with two aluminum electrodes (150 mm × 75 mm × 5 mm) maintaining a separation of 70 mm from each other and electrically isolated from rest of the vacuum chamber.

For carbon removing from Au surface, the sample was put in between the parallel plates. The surface of the sample is kept perpendicular with respect to parallel plate surfaces. A base pressure of 10^{-6} mbar was achieved in the process chamber using a turbo-molecular pump backed by a roots pump. Oxygen gas with a flow rate of 30 sccm was injected in the process chamber through a mass flow controller and a pressure

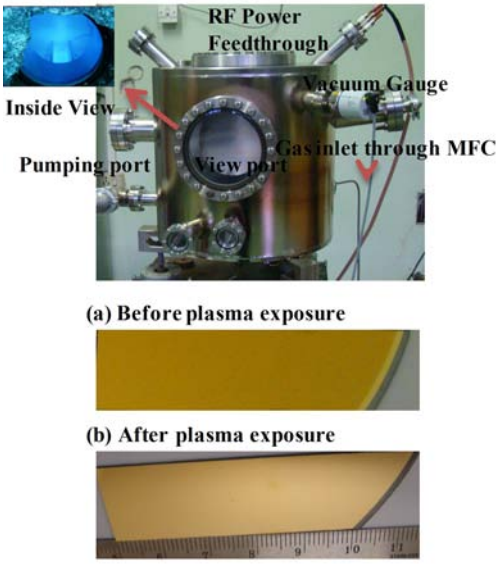

Fig. T.3.7: In-house developed capacitively coupled RF (13.56 MHz) plasma cleaning system is shown alongwith carbon coated Au sample before and after plasma exposure.

in 3-6×10^{-2} mbar range was maintained for plasma generation. A 13.56 MHz RF power supply (AG 0613: T&C Power Conversion) with automatic tuning network (AIT-600) was used for power feeding to electrodes. Photograph of RF plasma system is shown in Figure T.3.7. The 10 watt RF power (88 mW/cm^2) was fed to one of the electrode and the second electrode was kept at the ground potential. The sample was exposed for 20 minutes for complete removal of carbon. For cleaning applications it is very essential that the energy of ions should not increase up to the sputtering threshold of electrode material, otherwise sputtering from electrode surface will occur and that in turn will contaminate the surface of the object to be cleaned. The energy of ions can be controlled by self-bias voltage generated on power electrode. In present case, we have used symmetric electrode configuration (dimensions of both electrodes are kept the same) and the self-bias voltage is kept between 0 to 5 V by adjusting the RF power and process gas pressure in the system.

At these optimized parameters of RF plasma a carbon contaminated gold coated spherical mirror, which is used in reflectivity beamline (BL-03) of Indus-2, is cleaned. In order to avoid heating effect on mirror surface, the mirror was exposed to RF plasma in four successive stages for more than four hours. Images of mirror before and after cleaning are shown in Figure T.3.8.

3.1.2 IR laser scanning setup

Customized Yb-doped fiber laser system was used to remove carbon from gold surface. The laser has variable power (0-30 W) and pulse frequency (20-200 kHz). The laser system is equipped with galvanometric scanner which can scan 150 mm × 150 mm area in XY plane with scan speed (v_{scan}) from 50-8000 mm/s. To remove the carbon from gold surface a hatching pattern (0° - parallel to y = 0° line, 90° - parallel to x = 0° line and 45° - parallel to x = y line) in XY plane is chosen in such a way that maximum area can be scanned by the laser beam.

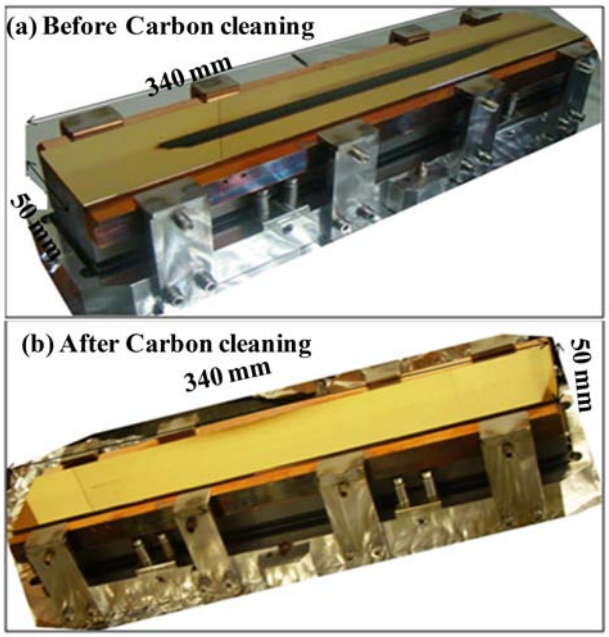

Fig. T.3.8: Gold coated spherical mirror (a) before and (b) after carbon cleaning using RF plasma exposure.

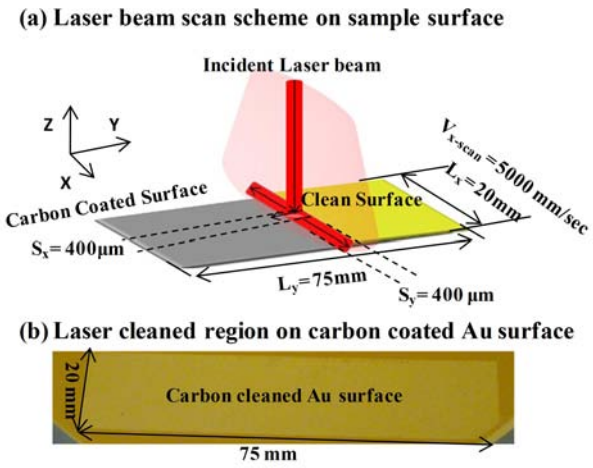

Fig. T.3.9: (a) Schematic of laser beam scanning. L_x and L_y represent sample length and width, S_x and S_y represent laser beam size in x and y- directions and $V_{x\text{-}scan}$ represents laser scan speed in x - direction (b) Laser cleaned region (20 mm×75 mm) of carbon coated Au sample surface.

The schematic of laser beam scanning on sample surface is shown in Figure T.3.9(a). For carbon cleaning a carbon coated gold sample was kept 5.5 mm above the focal plane of laser beam (5.5 mm above the focal plane the beam diameter is ~ 0.4 mm) in XY plane and the laser was operated at 30 W power, 90 kHz pulse frequency, 170 ns pulse width, scan speed ($V_{x\text{-}scan}$) = 5000 mm/s and V_y = 15 µm/scan. The fluence (0.26 J/cm^2) and number of beam scans on sample surface were decided by optimizing the system using test samples of carbon coated Au thin films. For complete removal of carbon, the laser beam scans the sample surface (in user defined pattern) twenty times, then for polishing purpose, sample is moved additional 3 mm above (away from focus, at reduced fluence) and the same scanning pattern was repeated for another ten times. The carbon cleaned region on carbon coated Au surface is shown in Figure T.3.9(b). Total time taken for removing carbon from sample is ~ 30 minutes.

3.1.3 UV radiation setup

Low pressure mercury lamp gives a discrete energy spectrum in which radiations of wavelengths below 253.7 nm are useful for carbon removal. Radiations of wavelength 253.7 nm break the bonds of organic molecules and 184.9 nm wavelength radiations dissociate the oxygen molecule into oxygen radicals. Oxygen radicals combine with molecular oxygen (O_2) and produce ozone (O_3) gas [12]. Ozone has large absorption cross section at 253.7 nm. Absorption of 253.7 nm wavelength by O_3 reduces its intensity, resultant cracking of contaminant molecule decreases consequently cleaning efficiency decreases [13]. For avoiding such limitations, for carbon cleaning from gold surface, a UV radiation source of 172 nm wavelength was used. Radiations of λ=172 nm (~7.2 eV) dissociate both organic molecule as well as oxygen molecule simultaneously[14].

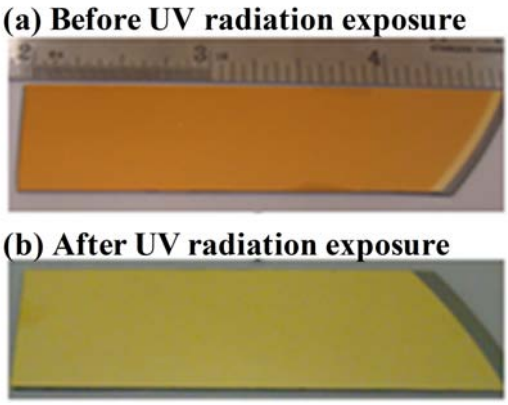

Fig. T.3.10: Carbon coated Au sample (a) before and (b) after UV radiation exposure.

In this setup, the carbon coated gold thin film sample was kept at pre optimized distance (4-5 mm) below the UV source and continuously irradiated by UV radiations for 7 hrs in ambient environment. Photographs of test samples before and after carbon removal from Au surface by UV radiation exposure is shown in Figure T.3.10. The intensity of UV radiation at UV lamp surface is ~ 50 mW/cm^2. The lamp system is equipped with an ozone decomposition unit, which exhausts the air from the enclosure at a rate of 0.26 m^3/min and reduces the O_3 spread in the surrounding environment.

4. Surface characterization before and after carbon cleaning

4.1 Soft x-ray reflectivity (SoXR)

In order to make the comparison of carbon removal efficiencies among various cleaning techniques, such as RF plasma, UV/O_3 and IR laser techniques, three identical samples of carbon coated Au thin film surfaces were independently treated with these techniques and their surfaces were characterized by surface analysis techniques.

Structural and optical characterization before and after carbon cleaning from Au surface were carried out using SoXR technique. Angle dependent reflectivity measurements were carried out using soft x-ray beam of 90 Å wavelength and energy dependent reflectivity measurements were performed in 100-300 eV energy range. SoXR data analyses were carried out using the Parratt formalism [15]. Figure T.3.11(a) shows experimentally measured and fitted angle dependent x-ray reflectivity curves of pristine Au thin film before and after carbon cleaning. In pristine carbon coated Au sample, the carbon layer causes modulated interference fringes and a shift in carbon critical angle towards lower angle side. In carbon cleaned samples, the critical angle position again restored to default value corresponding to Au layer and modulation in interference fringes also disappears.

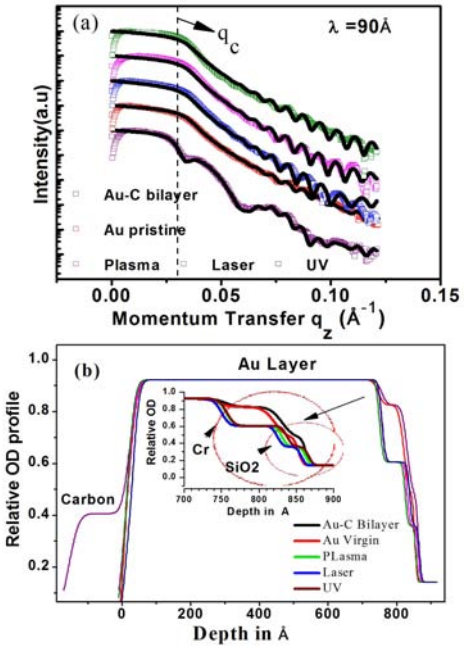

Fig. T.3.11: (a) Measured and fitted soft x-ray reflectivity spectra. (b) Relative optical density profile of carbon coated Au film, before and after carbon layer removal with UV, RF plasma and IR laser techniques.

Figure T.3.11(b) shows relative optical density (OD) of Au film before and after carbon layer removal using three different techniques as obtained from fitting of soft x-ray reflectivity curves. For soft x-ray data analyses a software code SRxrr [16] based on Parratt formalism [15] was used. First pristine Au sample parameters were determined, for data fitting values of optical constants of Si, SiO_2, Cr and Au are taken from Henke database [17]. During data fitting, optical constants (δ, β), thickness (t), roughness (σ) of SiO_2, Cr and Au were kept as free parameters. A 18.1 Å thin layer (δ=9.33E-3, β=1.02E-3) on top surface and a interface layer of SiO_2, of 32 Å thickness between Si substrate and Cr layer was considered for obtaining a best fit. The best fitted values of optical constants and structural parameters are shown in Table. T.3.1. The tabulated values clearly reveal that optical constants and thickness of Cr layer slightly vary after surface treatments but structural and optical parameters of Au layer remain nearly same after carbon cleaning by all three techniques. After removal of contamination layer it is observed that a thin layer of 19.7 to 26.8 Å thickness is formed on the Au top surface and the values of optical constants of this layer is different from the carbon layer.

Table T.3.1: Optical (δ, β) and structural (t, σ) parameters obtained by curve fittings of soft x-ray reflectivity of carbon coated Au film before and after carbon layer removal using RF plasma, UV and IR laser. Roughness (σ) and thickness (t) values are given in Angstrom (Å)

Layers	→	C	Au	Cr	SiO_2	Si-Bulk
Treatments						
Pristine Au	δ	0.00933	0.0335	0.03	0.017	0.0052
	β	0.00102	0.0093	0.015	0.017	0.016
	t	18.12	724	74.45	32.07	Bulk
	σ	7	18	12.51	12.41	5
Untreated Au/C	δ	0.0147	0.0335	0.030	0.017	0.0052
	β	0.00202	0.0093	0.015	0.017	0.016
	t	178	734	74.4	32.07	Bulk
	σ	23.3	18	12.5	12.41	5
UV Exposed Au/C	δ	0.00747	0.0335	0.022	0.013	0.0052
	β	0.00496	0.0093	0.015	0.169	0.016
	t	26.8	726	80.5	29	Bulk
	σ	8.95	15.15	8.31	6.21	5
RF plasma Exposed Au/C	δ	0.0212	0.0335	0.022	0.013	0.0052
	β	0.0048	0.0093	0.015	0.169	0.016
	t	25.6	726	74.4	32	Bulk
	σ	15.89	15.15	8.31	6.21	5
IR laser Exposed	δ	0.0182	0.0335	0.022	0.013	0.0052
	β	0.0048	0.0093	0.015	0.169	0.016
	t	19.7	726	74.4	32	Bulk
	σ	13.9	15.15	8.31	6.21	5

The top surface morphology of all the samples was also imaged by AFM measurements. The surface morphology clearly revels that after UV and plasma treatments the surface roughness values decrease from 24.0 Å to 16.0 Å and 8.0 Å respectively, whereas after laser treatment surface roughness increases from 24.0 Å to 56.0 Å.

Figure T.3.12 shows energy dependent reflectivity spectra measured in 100 to 300 eV energy range for pristine Au, carbon coated Au and carbon removed Au samples. The UV and plasma treated samples show a reflectivity gain in 100 to 300 eV energy range and the reflectivity of these samples also closely match with the pristine Au thin film reflectivity. The laser treated sample shows a loss in reflectivity compared to pristine Au as well as unexposed carbon coated Au surface. Due to overlap of carbon edge at 284 eV and destructive interference fringe the unexposed carbon coated Au sample shows a dip at 280 eV.

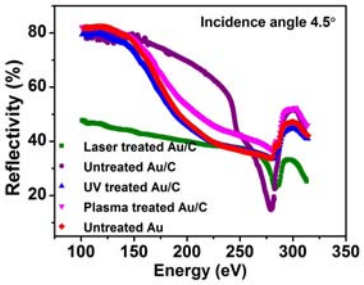

Fig. T.3.12: Energy dependent x-ray reflectivity spectra of pristine Au, carbon coated Au and after exposure with RF plasma, UV, IR laser setups.

4.2 X- ray photoelectron spectroscopy (XPS)

To see the chemical changes on Au surface after UV radiations, RF plasma and IR laser exposure on carbon coated Au surface, XPS experiments were carried out near carbon K-edge (1s) region (280 to 290 eV) at beamline BL-14 of Indus-2 synchrotron radiation source using photon energy 4.3 keV[18].

The original recorded spectra are fitted by deconvolution using "XPSPEAK" program. The deconvolution process included the subtraction of Shirley-type backgrounds from each spectrum and the fitting of XPS peaks with Gaussian (80%)-Lorentzian (20%) functions. The total integrated areas under C (1s) peak and area under C-C (284.7 eV), C-OH (286.1 eV) and C=O (288.2 eV) peaks are measured for exposed and unexposed samples. The ratios for each peak with respect to pristine Au sample are calculated and plotted in Figure T.3.13.

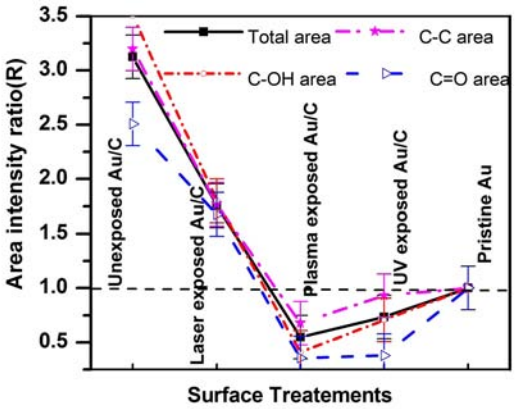

Fig. T.3.13: C (1s) peak area intensity ratio of unexposed Au/C, pristine Au, laser, plasma and UV exposed Au/C to pristine Au, as obtained from XPS curve fittings.

4.3 Raman spectroscopy (RS)

The result of angle dependent SoXR confirms removal of carbon from Au surface after applying all three techniques whereas the XPS spectra still show a presence of carbon in laser exposed sample of less concentration compared to unexposed carbon coated Au sample. In order to overcome this contradiction one more carbon sensitive tool (Raman spectroscopy) is used for confirmation of carbon presence. The Raman spectra from a pristine Au surface, carbon deposited Au surface and after carbon cleaning with three different techniques were recorded by Jobin Yvon Horiba LABRAM-HR instrument, having λ= 473 nm excitation source. The laser light was coupled to a single mode fiber for delivering light to the microscope. The Raman signal was collected using a 50X microscope objective and coupled to a 100 μm multimode optical fiber and the second end of multimode optical fiber is coupled to the spectrometer.

The Raman spectra from all the samples were acquired using TE cooled (-72 °C) CCD in the spectral region of 800 cm^{-1} to 1800 cm^{-1} at 1 cm^{-1} resolution. In order to avoid any heating damage on the sample surface, a low power beam (25 mW) of ~2 μm spot diameter on sample surface was used. Raman spectra from Au pristine sample, carbon coated Au and after carbon cleaning are shown in Figure T.3.14.

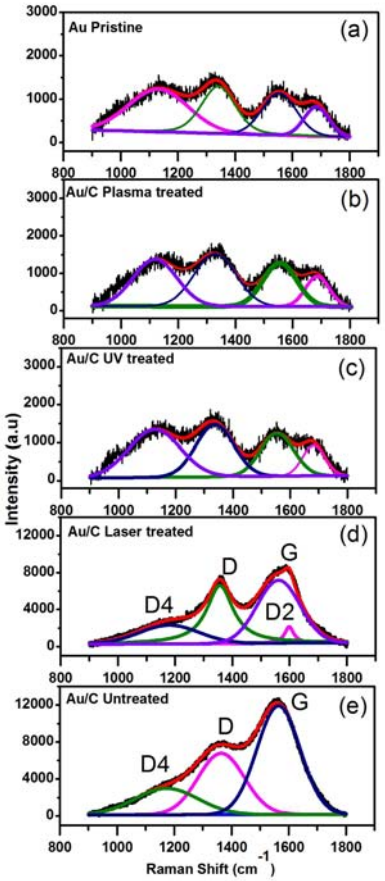

Fig. T.3.14: Measured and fitted Raman spectra of (a) Pristine Au (b) Plasma exposed (c) UV exposed (d) Laser exposed (e) Carbon coated Au. Various peaks (G, D, D2, D4) related to graphitic carbon are marked.

The Raman spectra of plasma and UV exposed samples match well to the pristine Au surface spectrum but laser exposed sample spectrum still shows a presence of carbon.

5. Discussions

Carbon layer from mirror-like Au surface is removed using three different techniques. In RF plasma technique, the carbon from Au surface is removed by synergetic effect of radical, electrons/ions and UV photons. The energetic particles (electrons, ions and photons) strike to the carbon containing surface and transfer the energy to the surface atoms/molecules, resultant C-C/C-H bonds break and dangling bonds are formed. The dangling bonds containing carbon atoms are highly reactive, subsequently they react with oxygen radicals present in the plasma and they form volatile gas species such as CO and CO_2. These gases are removed by dynamic gas pumping and a carbon free surface is obtained. In UV cleaning method, the UV radiations activate hydrocarbon molecules adsorbed on optics surface and simultaneously dissociate oxygen and ozone molecules into oxygen radicals in the vicinity of optics surface. The oxygen radicals react with activated hydrocarbon molecules and form volatile gaseous species, resultant a contamination free surface is obtained. In laser cleaning method the carbon from optics surface is removed by selective ablation process.

Due to large thermalization time (μs) of non-metals, nanoseconds (ns) pulsed laser increases the temperature of carbon layer by non thermal way (photochemical process); resultant sudden increase in temperature produces thermal expansion of top layer (contamination layer) [19]. By this thermal expansion force, contamination layer particles are ejected from the surface.

The carbon cleaned Au surface is characterized using different surface analyses techniques. The SoXR results reveal that carbon from Au surface is completely removed by all three techniques and surface roughness of Au does not increase after carbon removal. The reflectivity results show a presence of surface layer of low absorption coefficient on top surface of Au after carbon removal. The energy dependent reflectivity results (Figure T.3.12) reveal that after carbon removal using UV and RF plasma, the Au surface reflectivity in 100 to 300 eV energy range is well matched with the pristine Au surface, whereas laser exposed sample shows a reduction in reflectivity in this energy range. There may be two possible reasons by which reflectivity can reduce, (i) increase in surface roughness and (ii) presence of any other contamination layer on top surface of Au. In order to confirm surface morphology, AFM measurements were carried out. The AFM results reveal that after UV and plasma exposure rms roughness vary from 13 Å to 17 Å and 8 Å respectively, whereas for laser exposed sample rms roughness increased from 13 Å to 56 Å. The inconsistency in results of AFM and x-ray reflectivity (XRR) measurements is observed by other groups also [20], [21]. Lee et al. [20] obtained surface roughness variation in Mo thin films by AFM and XRR by more than five times. They concluded that low density particles cannot be detected by XRR whereas these particles are easily sensed by AFM in noncontact mode measurements.

In XPS spectra, the peak area intensity ratios clearly reveal that after carbon cleaning using RF plasma and UV radiation exposure, the carbon gets completely removed and carbon concentration on Au surface reduced to that of adsorbed hydrocarbons as present on pristine Au surface. On the other hand, in laser treated sample the area intensity ratio of all the peaks reduced significantly but it is still higher than the pristine Au sample as well as plasma and UV exposed samples.

The Raman spectra of UV radiations and RF plasma exposed samples are well matched with pristine Au sample spectrum (see Figure T.3.14). Presences of various low intensity peaks in Raman spectra of pristine as well as in UV and plasma exposed samples are due to ambient hydrocarbon gases adsorbed on the Au surface. The first order spectra of laser exposed sample and carbon coated untreated Au sample are fitted by peak fit program by considering mixed Lorentzian and Gaussian functions. In laser treated sample G and D bands of graphitic carbon with an additional band known as shoulder of D band at 1180 cm^{-1} (D4) are observed with reduced intensity compared to unexposed carbon coated Au sample. The G-band center is around 1560 cm^{-1} and is due to an ideal lattice vibration mode with E_{2g} symmetry and shows the presence of sp^2 hybridized carbon[22].

The D band indicates presence of disorder in carbon ring and is related to the breathing mode of the carbon hexagons. In laser exposed sample, splitting in G band into two bands G (1560 cm^{-1}) and D2 (1600 cm^{-1}) is observed. This type of splitting in graphitic carbon sample occurs due to random distribution of impurities, the localized vibrations mode of impurities interact with extended phonon modes of graphene [23]. Decrease in D band intensity indicates that number of carbon rings as well as disordering in given sample decrease. The D4 peak center around 1180 cm^{-1} is attributed to presence of sp^2-sp^3 mixed phase of carbon[24], [25].

The XPS and RS results show a presence of graphitic carbon after laser cleaning however its concentration is reduced with respect to carbon coated pristine gold sample. These results indicate that carbon is present on laser exposed sample surface and it is in the form of small clusters; these clusters are detected by XPS and RS measurements. In case of SoXR due to large area averaging the average absorption coefficient detected by reflectivity measurement is low compared to carbon absorption coefficient. In case of RF plasma and UV radiation exposures it is found that the carbon layer is completely removed. The AFM results indicate that after UV and plasma exposure surface roughness do not increase but in case of laser exposed sample surface roughness increases.

Conclusions

RF plasma, UV/O_3 and IR laser based three independent techniques are setup for refurbishing carbon contaminated synchrotron optics. For cross comparison of effects of these independent techniques on Au surface after carbon removal a systematic study is carried out on three identical carbon coated gold samples. After carbon layer removal by each technique these samples are characterized. Soft x-ray reflectivity results show a removal of carbon layer without increase in surface roughness with all three techniques. However, AFM results indicate that after laser treatment the surface roughness increases significantly. The SoXR technique suggests a presence of low density surface layer of ~ 20Å to 27 Å thickness after removal of main carbon layer. After laser treatment, the Raman spectroscopy and XPS results showed a signature of carbon on Au surface, most likely due to carbon present in form of particulates to which the SoXR technique is not sensitive. Enhancement in soft x-ray reflectivity near carbon K edge is observed after carbon removal by UV and plasma technique and the reflected intensity of these samples closely matches with the pristine Au thin film intensity. The laser treated sample also shows an increase in reflected intensity in carbon K-edge region but not upto pristine Au sample reflectivity level. Results of present study suggest that RF plasma and UV radiation techniques are useful for carbon cleaning applications. In case of IR laser technique, it seems that the carbon particulates resettled on the cleaned surface from the removal debris of carbon and therefore needs further process optimization.

Acknowledgements

The research and development work presented here is part of the Ph.D. thesis (under Homi Bhabha National Institute,

Mumbai) of the first author of this article, Dr. Praveen K. Yadav, Scientific Officer-F at RRCAT. The research work was performed under the guidance of Prof. Mohammed H. Modi, Scientific Officer-H, Head, Soft X-ray Applications Laboratory, Synchrotrons Utilization Section.

The authors gratefully acknowledge Shri S.V. Nakhe, Director, RRCAT for support, encouragement and keen interest in the carbon cleaning activity. Support of Dr. Tapas Ganguli, Head, SUS and all members of SUS is gratefully acknowledged. Thanks are due to Dr. J. A. Chakera, Head, LPD, Dr. M. Kumar, Dr. A. Choubey and Mr. Sabir Ali for their help and support in this activity.

References

[1] D. H. Bilderback, P. Elleaume, and E. Weckert, "Review of third and next generation synchrotron light sources," J. Phys. B: At. Mol. Opt. Phys. vol. 38, pp. 773–797, 2005.

[2] M. Yabashi, K. Tono, H. Mimura, S. Matsuyama, K. Tanaka, T. Yamauchi, H. Tanaka, K. Tamasaku, H. Ohashi, S. Goto, and T. Ishikawa, "Optics for coherent X-ray applications," J. Synchrotron Rad. vol. 21, pp. 976-985, 2014.

[3] J. Hollenshead and L. Klebanoff, "Modeling radiation-induced carbon contamination of extreme ultraviolet optics," J. Vac. Sci. Technol. B Microelectron. Nanom. Struct., vol. 24, pp. 64–82, 2006.

[4] K. Boller, R. P. Haelbich, H. Hogrefe, W. Jark and C. Kunz, "Investigation of carbon contamination of mirror surfaces exposed to synchrotron radiation", Nucl. Instrum. Methods Phys. Res, vol. 208, pp. 273–279, 1983.

[5] A.C. Ferrari And J. Robertson, "Raman spectroscopy of amorphous, nanostructured, diamond-like carbon, and nanodiamond," Phil. Trans. R. Soc. Lond. vol. 2, pp. 2477–2512, 2004.

[6] P. K. Yadav, R. K. Gupta, M. K. Swami, and M. H. Modi, "Structural variation in a synchrotron-induced contamination layer (a-C:H) deposited on a toroidal Au mirror surface," J. Synchrotron Rad., vol. 24, pp. 757–764, 2017.

[7] C. Chauvet F. Polack, M. G. Silly, B. Lagarde, M. Thomasset, S. Kubsky, J. P. Duval, P. Risterucci, B. Pilette, I. Yao, N. Bergeard and F. Sirotti, "Carbon contamination of soft X-ray beamlines: Dramatic anti-reflection coating effects observed in the 1 keV photon energy region", J. Synchrotron Rad., vol. 18, pp. 761–764, 2011.

[8] R. V. Nandedkar, K. J. S. Sawhney, G. S. Lodha, A. Verma, V. K. Raghuvanshi, A. K. Sinha, M. H. Modi and M. Nayak, "First results on the reflectometry beamline on Indus-1," Curr. Sci., vol. 82, pp. 298–304, 2002.

[9] P.J. Singh, A. Shastri, R. S. Kumar, S.N. Jha, S.V.N.B. Rao, R. D'Souza and B.N. Jagatap, "First commissioning results from high resolution vacuum ultraviolet beamline at Indus-1 synchrotron source," Nucl. Instruments Methods in Phys. Res. A vol. 634, pp. 113–119, 2011.

[10] P. K. Yadav, M. H. Modi, M. K. Swami, and P. J. Singh, "Ex-situ characterization of synchrotron radiation induced carbon contamination on LiF window," J. Electron Spectros. Relat. Phenomena, vol. 211, pp. 64–69, 2016.

[11] P. K. Yadav, M. Kumar, R. K. Gupta, M. Sinha, J. A. Chakera, and M. H. Modi, "Refurbishment of an Au-coated toroidal mirror by capacitively coupled RF plasma discharge," J. Synchrotron Rad., vol. 26, pp. 1152–1160, 2019.

[12] J. R. Vig, "UV / ozone cleaning of surfaces," J. Vac. Sci. Technol. A, vol. 3, pp. 1027–1034, 1985.

[13] Z. Falkenstein, "Surface cleaning mechanisms utilizing VUV radiation in oxygen containing gaseous environments" Proc. SPIE, vol. 4440, pp. 246–255, 2001.

[14] K. Tanaka, K. Hamamoto, N. Sakaya, M. Hosoya, T. Watanabe and H. Kinoshita, "Cleaning characteristics of contaminated imaging optics using 172 nm radiation", Jpn. J. Appl. Phys.,vol. 46, pp. 6150–6154, 2007.

[15] L. G. Parratt, "Surface Studies of Solids by Total Reflection of X-Rays," Phys. Rev., vol. 95, pp. 359–369,1954.

[16] M. H. Modi, G. S. Lodha, and and M. I. P. Mercere, "Live simulator and data analysis tool for multilayer reflectivity using LabVIEWtle." The 9th International Conference on the Physics of X-Ray Multilayer Structures, Big Sky Resort USA, 2008.

[17] The centre of optics (CXRO) at Berkeley National Laboratory, Berkeley, CA, USA. Berkeley, [Online]. Available: http:// henke.lbl.gov/optical_constant/layer2.html.

[18] Jagannath, U. K. Goutam, R. K. Sharma, J. Singh, K. Dutta, U. S. Sule, R. Pradeep and S. C. Gadkari,"HAXPES beamline PES-BL14 at the Indus-2 synchrotron radiation source", J. Synchrotron Rad., vol. 25, pp. 1541–1547, 2018.

[19] D. Bäuerle, Laser Processing and Chemistry, 3rd edn. Berlin: Heidelberg, 2000.

[20] C. H. Lee, F.G. Guo and C.C. Chu, "The thickness dependent of optical properties, resistance, strain and morphology of Mo thin films for the back contact of CIGS solar cells", Chin. J. Phys., vol. 50, pp. 311-321, 2012.

[21] H. C. Su, C. H. Lee, M. Z. Lin, and T.W. Huang., "A comparison between X-ray reflectivity and atomic force microscopy on the characterization of a surface roughness", Chin. J. Phys., vol. 50, pp. 291-300, 2012.

[22] C. Casiraghi, F. Piazza, A. C. Ferrari, D. Grambole, and J. Robertson, "Bonding in hydrogenated diamond-like carbon by Raman spectroscopy," Diam. Relat. Mater., vol. 14, pp. 1098–1102, 2005.

[23] A. C. Ferrari, "Raman spectroscopy of graphene and graphite: Disorder, electron–phonon coupling, doping and nonadiabatic effects," Solid State Communication. vol. 143, pp. 47–57, 2007.

[24] B. Dippel, H. Jander, and J. Heintzenberg, "NIR FT Raman spectroscopic study of Ñame soot," Phys. Chem. Chem. Phys., vol. 1, pp. 4707–4712, 1999.

[25] A. Sadezky, H. Muckenhuber, H. Grothe, R. Niessner and U. Pöschl, "Raman microspectroscopy of soot and related carbonaceous materials: Spectral analysis and structural information," Carbon. vol. 43, pp. 1731-1742, 2005.